GEOPHYSICAL RESEARCH LETTERS, VOL. 35, L15804, doi:10.1029/2008GL034058, 2008

Correlation of secondary organic aerosol with odd oxygen in Mexico City

Scott C. Herndon,[1] Timothy B. Onasch,[1] Ezra C. Wood,[1] Jesse H. Kroll,[1]
Manjula R. Canagaratna,[1] John T. Jayne,[1] Miguel A. Zavala,[2,3] W. Berk Knighton,[4]
Claudio Mazzoleni,[5] Manvendra K. Dubey,[5] Ingrid M. Ulbrich,[6] Jose L. Jimenez,[6]
Robert Seila,[7] Joost A. de Gouw,[8] Benjamin de Foy,[9] Jerome Fast,[10] Luisa T. Molina,[2,3]
Charles E. Kolb,[1] and Douglas R. Worsnop[1]

Received 22 March 2008; revised 7 May 2008; accepted 20 June 2008; published 5 August 2008.

[1] Photochemically processed urban emissions were characterized at a mountain top location, free from local sources, within the Mexico City Metropolitan Area. Analysis of the Mexico City emission plume demonstrates a strong correlation between secondary organic aerosol and odd oxygen ($O_3 + NO_2$). The measured oxygenated-organic aerosol correlates with odd oxygen measurements with an apparent slope of (104–180) μg m^{-3} $ppmv^{-1}$ (STP) and $r^2 > 0.9$. The dependence of the observed proportionality on the gas-phase hydrocarbon profile is discussed. The observationally-based correlation between oxygenated organic aerosol mass and odd oxygen may provide insight into poorly understood secondary organic aerosol production mechanisms by leveraging knowledge of gas-phase ozone production chemistry. These results suggest that global and regional models may be able to use the observed proportionality to estimate SOA as a co-product of modeled O_3 production until more complete models of SOA formation become available. **Citation:** Herndon, S. C., et al. (2008), Correlation of secondary organic aerosol with odd oxygen in Mexico City, *Geophys. Res. Lett.*, *35*, L15804, doi:10.1029/2008GL034058.

1. Introduction

[2] Organic aerosol makes up a large fraction of atmospheric fine particulate matter, and thus has important implications for climate, health, and visibility. A substantial fraction of organic particulate matter is secondary organic aerosol (SOA), from the formation of low-volatility products of the atmospheric oxidation of volatile organic compounds (VOCs) [*Seinfeld and Pankow*, 2003]. SOA has been observed to increase rapidly in urban outflows [*Kleinman et al.*, 2007] and apparent rates of SOA production in urban outflows and urban atmospheres are far greater than current photochemical models predict [*de Gouw et al.*, 2005; *Volkamer et al.*, 2006].

[3] In the last several years, aerosol mass spectrometry has yielded substantial insight into the composition and abundance of atmospheric organic aerosol. Multivariate analysis techniques have been used to deconvolve complex organic mass spectra into smaller sets of chemically meaningful classes [*Zhang et al.*, 2005a; *Lanz et al.*, 2007; *Ulbrich et al.*, 2008]. Oxygenated organic aerosol (OOA), which is ubiquitous in the atmosphere, is associated with SOA, whereas hydrocarbon-like organic aerosol (HOA), which is found in highest quantities in urban environments, is attributed to primary organic aerosol (POA) from combustion sources [*Zhang et al.*, 2005b, 2007]. The high levels of OOA [e.g., *Volkamer et al.*, 2006] provide direct observational evidence of the need to better describe the sources and mechanisms of SOA formation in regional and global models. In this work we show that in the outflow of a megacity (Mexico City), OOA and photochemical oxidant production are strongly correlated, suggesting that SOA may be viewed as a co-product of modeled O_3 production.

2. Measurement and Analysis Description

[4] This article describes data collected at Pico de Tres Padres (PTP), the highest point in the Sierra de Guadalupe range in the northern section of the MCMA. It rises ~700 meters above the surrounding city and has very few local emission sources. The mobile laboratory deployment site selection was guided by forecast models and the detailed basin flow response to different synoptic scale forcings developed by *de Foy et al.* [2005] during the MCMA-2003 campaign. A topographical map showing the MCMA area and the sites described above is included as auxiliary material[1].

[5] Based on the measurements of boundary-layer depths measured at two super-sites in Mexico City [*Shaw et al.*, 2007] the following qualitative statements can be drawn about the structure of the lower atmosphere on a typical day.

---

[1] Aerodyne Research, Inc., Billerica, Massachusetts, USA.
[2] Massachusetts Institute of Technology, Cambridge, Massachusetts, USA.
[3] Molina Center for Energy and the Environment, La Jolla, California, USA.
[4] Department of Chemistry and Biochemistry, Montana State University, Bozeman, Montana, USA.
[5] Earth and Environmental Sciences Division, Los Alamos National Laboratory, Los Alamos, New Mexico, USA.
[6] Department of Chemistry and Biochemistry and CIRES, University of Colorado, Boulder, Colorado, USA.
[7] National Exposure Research Laboratory, Environmental Protection Agency, Research Triangle Park, North Carolina, USA.
[8] Earth System Research Laboratory, NOAA, Boulder, Colorado, USA.
[9] Department of Earth and Atmospheric Sciences, Saint Louis University, St. Louis, Missouri, USA.
[10] Pacific Northwest National Laboratory, Richland, Washington, USA.

0094-8276/08/2008GL034058$05.00

[1] Auxiliary materials are available in the HTML. doi:10.1029/2008GL034058.

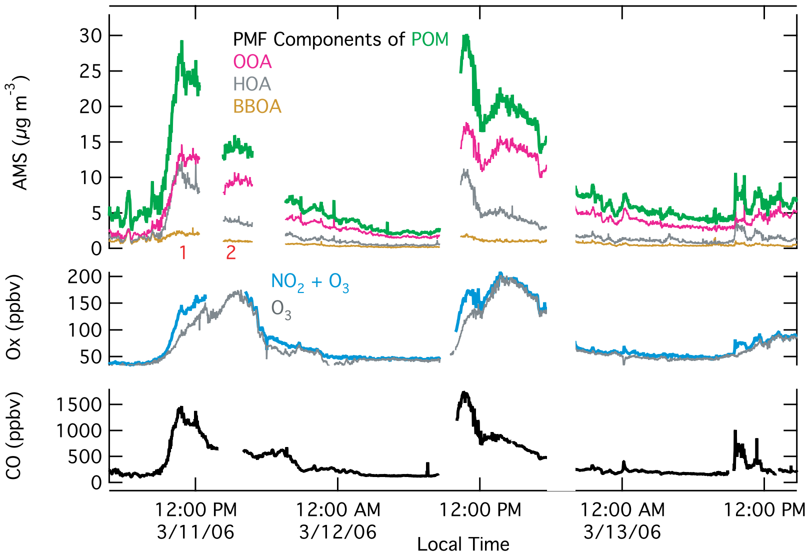

Figure 1. Time series of AMS and Gas-Phase Data at PTP. (bottom) The carbon monoxide mixing ratio is depicted versus local time at PTP. (middle) The light grey trace is the measured O_3 and the cyan blue trace is O_X (= $NO_2 + O_3$). (top) The total particulate organic matter (<1μm) is in green. The mass loading is at ambient conditions. The positive matrix factorization components of the organic matter are depicted; OOA (pink), HOA (grey) and BBOA (brown). The labels "1" and "2" are discussed in the text.

During clear-sky insolation, the mixed layer grew to a height of ~1 km above the basin floor by 11:30 local time. Upslope winds frequently brought Mexico City pollution to the PTP site at least 30 minutes before the mixed layer depth grew above the site elevation. The mixed layer rose to 2–4 km above the basin floor by the middle of each afternoon.

[6] The combination of mixed layer growth, altitude, and proximity to Mexico City made PTP's location ideal to sample urban outflow after mid-morning without being strongly influenced by local sources. The horizontal transport timescale to the nearest road is on the order of 15 – 60 minutes (assuming wind speeds <5 m s^{-1}) while the transport time from other parts of the city is on the order of hours. In contrast, the vertical mixing time scale is expected to be less than 30 minutes [*Stull*, 1988]. The analysis of mixing layer heights, coarse transport simulations and CO measurements suggest that the air reaching the PTP site represents the mixed urban plume.

[7] In this analysis, particulate mass loadings from an Aerodyne Aerosol Mass Spectrometer (AMS) [*Canagaratna et al.*, 2007] are correlated with various gas-phase measurements. CO and NO_2 were measured using tunable infrared laser differential absorption spectroscopy using a pulsed quantum cascade laser light source [*Herndon et al.*, 2005]. Ozone was measured using a 2B Technologies Model 205 dual beam ozone monitor. Selected volatile organic carbon (VOC) species were measured using proton transfer reaction mass spectrometry (PTR-MS) [*Rogers et al.*, 2006]. Evacuated canisters were used to collect whole air samples for off-line analysis of the composition of the VOCs using gas-chromatographic methods during selected 20 minute sampling intervals throughout the campaign. Positive matrix factorization (PMF) was used to deconvolve the complex organic fragments in the particle mass spectra [*Lanz et al.*, 2007; *Ulbrich et al.*, 2008] into hydrocarbon-like organic aerosol (HOA), oxygenated organic aerosol (OOA) and biomass burning organic aerosol (BBOA).

[8] Typically, at night the site measured pollutants within the residual layer since the inversion level remained below the sampling altitude. In the absence of fresh emissions or trapped residual layers advected to the sampling location, the nighttime mixing ratios of CO and O_3 were 125 ± 6 ppbv and 44 ± 3 ppbv, respectively. The organic PM 'background' loading at night was 1.1 ± 0.4 μg m^{-3} (STP, 273 K and 1 atm) and was dominated by the most oxidized form of OOA.

[9] A measure of the extent of atmospheric oxidation of emitted VOCs can be quantified from the ratios of hydrocarbon species with dissimilar reactivities toward OH [*Roberts et al.*, 1984]. The attribution of a single photochemical time to an urban air mass is not well defined when fresh emissions are entrained [*Parrish et al.*, 2007]. An effective photochemical age, Δt[OH] can be computed using measurements of the C9 aromatic species and benzene. This qualitative metric is appropriate for the measurements at PTP due to the relatively short atmospheric lifetime of the C9 aromatics; 3–12 hours for the measured OH concentrations at an urban supersite by *Dusanter et al.* [2008]. The quantity Δt[OH] can be heavily influenced by mixing and transport; in the context here it is an estimate of the extent of atmospheric processing.

3. Results and Discussion

3.1. Correlation of Organic Matter Composition With Gas-Phase Tracers

[10] Figure 1 depicts a two-day time series for selected data collected at PTP. The gas-phase species in Figure 1 are CO, O_3 and odd oxygen ($O_X = O_3 + NO_2$). The particulate organic matter is also shown, along with the main components arising from PMF analysis of the organic signal

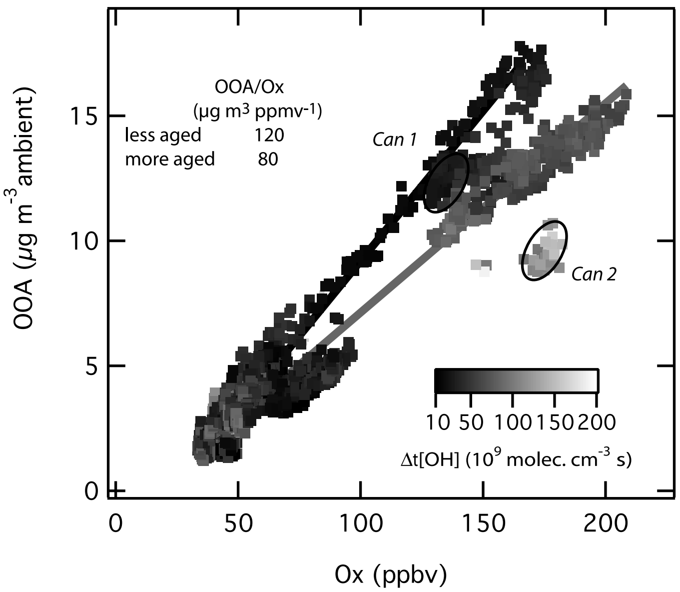

Figure 2. OOA versus O_X. The oxidized fraction of organic mass loading, OOA is depicted versus the sum of O_3 and NO_2 for the two-day period depicted in a previous figure. The square points have been inversely shaded by the extent of photochemical processing (Δt[OH]) calculated using the measurements of the C9-, C8- aromatic and benzene compounds described in the text. The slopes of the two lines are tabulated in the inset as 'less aged' and 'more aged' in ambient units. The circled points, labeled *Can 1* and *Can 2* refer to periods when GC VOC analysis were performed and are discussed in the text and in Figure 3.

described below. Events dominated by biomass-burning signatures are not included in this analysis. The other two organic aerosol components correlate with gas-phase tracers. Figure 1 shows a clear correlation of HOA with CO (both primary emissions) and OOA with O_X (both secondary pollutants).

[11] Qualitatively, HOA mass loadings are dominated by directly emitted organic aerosol [*Lanz et al.*, 2007; *Zhang et al.*, 2005b]. This analysis does not make a distinction between transportation emissions (e.g. diesel) and other sources which are not well represented in the primary biomass burning organic aerosol signature (BBOA) also shown in Figure 1. The HOA to CO ratio observed at PTP was 12 ± 1.5 μg m^{-3} ppmv^{-1} (STP).

[12] OOA correlates well with odd oxygen. During periods of photochemical production of organic aerosol, previous studies have reported correlation between O_3 and OOA [*Zhang et al.*, 2005b; *Volkamer et al.*, 2006; *Lanz et al.*, 2007], while little correlation is observed for periods dominated by multi-day regional transport and accumulation of OOA [*Zhang et al.*, 2005b]. O_X is a more conserved tracer of the extent of photochemical processing in the urban atmosphere than O_3 alone, because fresh emissions of NO react with O_3 to form NO_2. O_X is long-lived - its major loss mechanism on the time scales observed at PTP is the oxidation of NO_2 to form higher nitrogen oxides such as HNO_3 and PAN. We estimate that integrated O_X losses in the air masses observed are less than 20% of [O_X] based on measurements of NO_Z and calculations of other O_X losses.

3.2. OOA/O_X and Photochemical Processing

[13] In Figure 2, the OOA mass loading is plotted vs. the O_X concentration. The data in this figure is from the same time period shown in Figure 1. The shading is the calculated photochemical age, Δt[OH]. These data show two distinct clusters which are classified as "less aged" or "more aged" and are well defined using a threshold Δt[OH] value of 40×10^9 molecules cm^{-3} s. The slope of OOA/O_X for the "less aged" set of points is greater than the "more aged" set of points.

[14] The correlation between SOA and O_X is now examined in terms of the production rates of each. Odd oxygen (ozone) is formed by the atmospheric processing of emitted urban VOCs in the presence of NO_x. Under the conditions in air above MCMA, the rate of O_3 production [*Kleinman et al.*, 2002] is:

$$p(O_3) \approx \Sigma k_i a_i [OH][VOC]_i \qquad (1)$$

where the production rate of ozone is estimated by summing the contributions from individual VOC compounds. In (1), k_i is the rate coefficient for the reaction of OH with each specific VOC and a_i is a stoichiometric factor that depends on each specific VOC.

[15] The atmospheric oxidation of gas-phase organics also leads to the production of SOA, via the formation of low-volatility oxidation products [e.g., *Seinfeld and Pankow*, 2003]. At the PTP site, the oxidation of most VOC species is dominated by reaction with OH; oxidation by NO_3 is unlikely to be dominant during the daytime, and observations of SOA formation in the absence of O_3 (during which time O_X is dominated by NO_2) suggest that SOA formation from O_3-initiated oxidation is also relatively unimportant. Assuming the formation of semi-volatile compounds from the oxidation of VOCs is the rate limiting step in the formation of SOA [*Lim and Ziemann*, 2005;

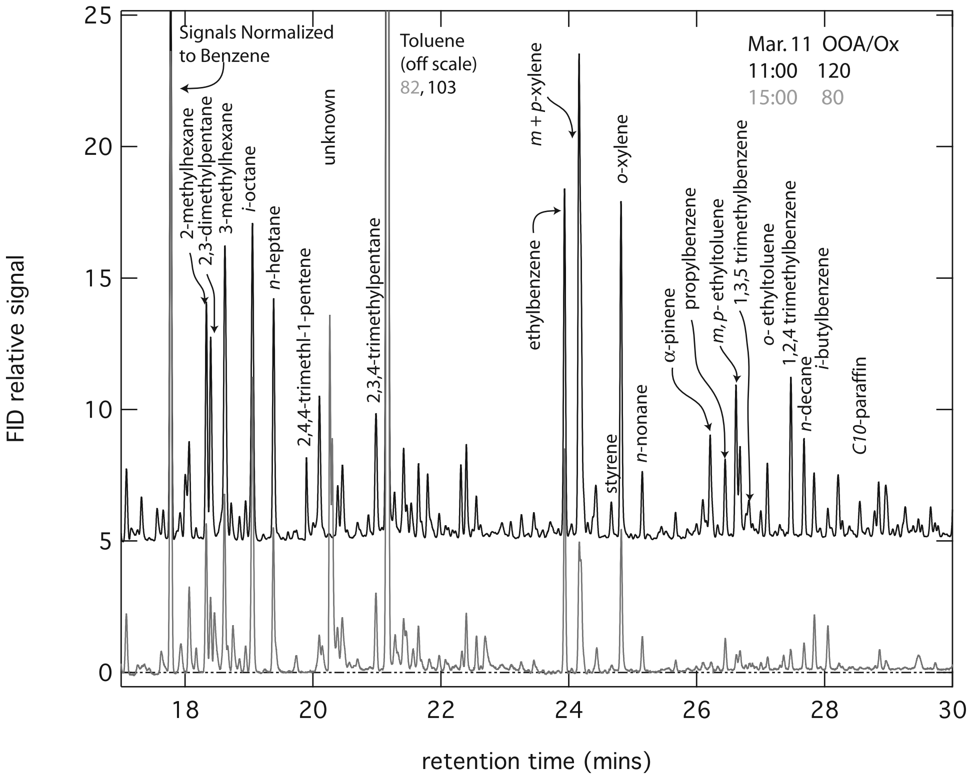

Figure 3. GC-FID Chromatograms for two time periods on 3/11 at PTP. The black trace is the chromatogram for the early morning canister sample and the grey trace is more photochemically processed air. The black less aged chromatogram has been offset 5 units for visual clarity. The two chromatograms have been normalized for dilution by equating the area of the benzene signal. Note that toluene is off-scale for both chromatograms with the numbers 82 and 103 indicating the peak height in units of relative FID signal.

Ng et al., 2007] then an expression for p(SOA) will resemble equation 1, with a_i representing the SOA yield from a given VOC.

[16] This analysis assumes that the observed OOA and O_X increase via chemistry only and that there are no significant losses of either OOA or O_X on the time-scale of these measurements (1–15 hours). With these caveats in mind, we relate the observed ratio to a simple expression based solely on the production terms,

$$\frac{\Delta \mathrm{OOA}}{\Delta \mathrm{O_x}} \approx \frac{\int p(\mathrm{SOA})dt}{\int p(\mathrm{O_3})dt} \qquad (2)$$

where the delta quantities on the left-hand side of the equation are increases in each attributed to the atmospheric processing of urban emissions and the integrals on the right-hand side represent the formal mechanism by which OOA and O_X increase respectively.

3.3. VOC Composition, Dependence of ΔOOA/ΔO_X

[17] The observed change in the slope of ΔOOA/ΔO_X (Figure 2) with photochemical age is due to a decrease in p(SOA) and/or an increase in $p(O_3)$ as the VOC mixture ages. Chromatograms from the GC analysis of two sample canisters taken on 3/11/2006 are depicted in Figure 3. The first sample (black trace), was collected for 20 minutes during the 11:00 hour and the second (grey trace) during the 15:00 hour (these times are highlighted in Figures 1 and 2). The raw chromatograms have been normalized for dilution using benzene. The black trace lies along the 'less aged' slope in Figure 2 while the grey trace is 'more aged'. The compounds shown, mostly aromatics and alkanes with six or more carbons, are substantially depleted (by ~50% on average) in the "more aged" sample due to photochemical processing. As these large organic compounds are expected to dominate SOA formation, further photochemical processing of such a sample may lead to lower production of SOA. However, even though the larger hydrocarbons are significantly depleted, the smaller hydrocarbons (C5 and lower, not shown) do not change dramatically. These smaller hydrocarbons account for a dominant fraction (>80% by number) of the total (nonmethane) hydrocarbon OH reactivity. As a result, O_3 formation is not expected to change as dramatically as SOA formation, and the likely result of the change in hydrocarbon mix over the course of the day is the observed decrease in the ΔOOA/ΔO_X ratio.

[18] The decrease in SOA production (relative to O_3 production) as the VOC mixture ages is most likely attributable to the decrease in concentrations of relatively large (C6 and greater) hydrocarbons. This is consistent with laboratory studies of SOA formation; aromatics have long been recognized as an important anthropogenic SOA precursor [e.g., *Ng et al.*, 2007; *Odum et al.*, 1997, and references within], and recent work has shown that long-chain alkanes may be major contributors as well. *Lim and Ziemann* [2005] have shown that for some SOA precursor alkanes, OH-initiated oxidation in the presence of NO_x

rapidly produces condensable matter in high (>50%) yields. *Robinson et al.* [2007] showed that photochemical processing of diesel exhaust produces significant secondary organic aerosol above what could be predicted based upon aromatic compounds only, strongly suggesting an important role for larger alkanes as a source of anthropogenic SOA.

[19] We note that the present discussion of the impact of VOC precursors on observed ΔOOA/ΔO_X ignores a number of detailed factors which may also influence the production of SOA and/or O_X, including multiple oxidation steps, temperature, [NO_x] and available particulate organic mass (M_0). The lower temperatures of the late night, presunrise morning periods may be influencing the OOA/O_X ratio in the locus of points defining the background OOA and O_X in Figure 2.

4. Summary and Implications

[20] This paper describes the observation of a strong correlation between SOA and O_X in photochemically processed urban outflow emissions measured in the MCMA. Preliminary analysis suggests that differences in observed OOA/O_X are driven in part by precursor VOC concentrations and will be the subject of detailed analysis in future work. This dataset provides valuable insights into the first few hours of mixing and oxidation of pollutant emissions from a large megacity.

[21] There is a need to develop computationally efficient treatments of the production of secondary organic aerosol in regional and global models. This work suggests that the production of regional SOA from anthropogenic emissions might be treated using a simple correlation with the production of O_3 until the anthropogenic VOCs are strongly attenuated via atmospheric processing. Although the correlation of OOA with O_X needs to be examined for other urban mixtures before more general conclusions can be formed, this approach may offer insight into investigations of *p*(SOA) using atmospheric observations.

[22] **Acknowledgments.** We gratefully acknowledge logistical assistance from Rafael Ramos. We would like to thank Manuel Quiñones of Televisa for providing power and on-site support. This work was funded in part by NSF grants (ATM-528227 and ATM-0528170) and DOE grants (DE-FGO2-05ER63982 and DE-FGO2-05ER63980). The United States Environmental Protection Agency through its Office of Research and Development collaborated in the research described here. It has been subjected to Agency review and approved for publication.

References

Canagaratna, M. R., et al. (2007), Chemical and microphysical characterization of ambient aerosols with the aerodyne aerosol mass spectrometer, *Mass Spectrom. Rev.*, *26*, 185–222.

de Foy, B., E. Caetano, V. Magaña, A. Zitácuaro, B. Cárdenas, A. Retama, R. Ramos, L. T. Molina, and M. J. Molina (2005), Mexico City basin wind circulation during the MCMA-2003 field campaign, *Atmos. Chem. Phys.*, *5*, 2267–2288.

de Gouw, J. A., et al. (2005), Budget of organic carbon in a polluted atmosphere: Results from the New England Air Quality Study in 2002, *J. Geophys. Res.*, *110*, D16305, doi:10.1029/2004JD005623.

Dusanter, S., D. Vimal, P. S. Stevens, R. Volkamer, and L. T. Molina (2008), Measurements of OH and HO_2 concentrations during the MCMA-2006 field campaign: Part 1. Deployment of the Indiana university laser-induced fluorescence instrument, *Atmos. Chem. Phys. Discuss.*, in press.

Herndon, S. C., et al. (2005), Characterization of urban pollutant emission fluxes and ambient concentration distributions using a mobile laboratory with rapid response instrumentation, *Faraday Discuss.*, *130*, 327–339.

Kleinman, L. I., P. H. Daum, D. Imre, Y.-N. Lee, L. J. Nunnermacker, S. R. Springston, J. Weinstein-Lloyd, and J. Rudolph (2002), Ozone production rate and hydrocarbon reactivity in 5 urban areas: A cause of high ozone concentration in Houston, *Geophys. Res. Lett.*, *29*(10), 1467, doi:10.1029/2001GL014569.

Kleinman, L. I., et al. (2007), Aircraft observations of aerosol composition and aging in New England and Mid-Atlantic States during the summer 2002 New England Air Quality Study field campaign, *J. Geophys. Res.*, *112*, D09310, doi:10.1029/2006JD007786.

Lanz, V. A., M. R. Alfarra, U. Baltensperger, B. Buchmann, C. Hüglin, and A. S. H. Prévôt (2007), Source apportionment of submicron organic aerosols at an urban site by factor analytical modelling of aerosol mass spectra, *Atmos. Chem. Phys.*, *7*, 1503–1522.

Lim, Y. B., and P. J. Ziemann (2005), Products and mechanism of secondary organic aerosol formation from reactions of n-alkanes with OH radicals in the presence of NOx, *Environ. Sci. Technol.*, *39*, 9229–9236.

Ng, N. L., J. H. Kroll, A. W. H. Chan, P. S. Chhabra, R. C. Flagan, and J. H. Seinfeld (2007), Secondary organic aerosol formation from m-xylene, toluene, and benzene, *Atmos. Chem. Phys.*, *7*, 4085–4126.

Odum, J. R., T. P. W. Jungkamp, R. J. Griffin, R. C. Flagan, and J. H. Seinfeld (1997), The atmospheric aerosol-forming potential of whole gasoline vapor, *Science*, *276*, 96–99.

Parrish, D. D., A. Stohl, C. Forster, E. L. Atlas, D. R. Blake, P. D. Goldan, W. C. Kuster, and J. A. de Gouw (2007), Effects of mixing on evolution of hydrocarbon ratios in the troposphere, *J. Geophys. Res.*, *112*, D10S34, doi:10.1029/2006JD007583.

Roberts, J. M., F. C. Fehsenfeld, S. C. Liu, M. J. Bollinger, C. Hahn, D. L. Albritton, and R. E. Sievers (1984), Measurements of aromatic hydrocarbon ratios and NOx concentrations in the rural troposphere: Estimates of air mass photochemical age and NOx removal rate, *Atmos. Environ.*, *18*, 2421–2432.

Robinson, A. L., N. M. Donahue, M. K. Shrivastava, E. A. Weitkamp, A. M. Sage, A. P. Grieshop, T. E. Lane, J. R. Pierce, and S. N. Pandis (2007), Rethinking organic aerosols: Semivolatile emissions and photochemical aging, *Science*, *315*, 1259–1262.

Rogers, T. M., et al. (2006), On-road measurements of volatile organic compounds in the Mexico City metropolitan area using proton transfer reaction mass spectrometry, *Int. J. Mass Spectrom.*, *252*, 26–37.

Seinfeld, J. H., and J. F. Pankow (2003), Organic atmospheric particulate material, *Annu. Rev. Phys. Chem.*, *54*, 121–140.

Shaw, W. J., M. S. Pekour, R. L. Coulter, T. J. Martin, and J. T. Walters (2007), The daytime mixing layer observed by radiosonde, profiler and lidar during MILAGRO, *Atmos. Chem. Phys. Discuss.*, *7*, 15,025–15,065.

Stull, R. B. (1988), *An Introduction to Boundary Layer Meteorology*, Kluwer Acad., Dordrecht, Netherlands.

Ulbrich, I. M., M. Canagaratna, Q. Zhang, D. R. Worsnop, and J. L. Jimenez (2008), Interpretation of organic components from positive matrix factorization of aerosol mass spectrometric data, *Atmos. Chem. Phys. Discuss.*, *8*, 6729–6791.

Volkamer, R., J. L. Jiménez, F. San Martini, K. Dzepina, Q. Zhang, D. Salcedo, L. T. Molina, D. R. Worsnop, and M. J. Molina (2006), Secondary organic aerosol formation from anthropogenic air pollution: Rapid and higher than expected, *Geophys. Res. Lett.*, *33*, L17811, doi:10.1029/2006GL026899.

Zhang, Q., M. R. Alfarra, D. R. Worsnop, J. D. Allan, H. Coe, M. R. Canagaratna, and J. L. Jiménez (2005a), Deconvolution and quantification of hydrocarbon-like and oxygenated organic aerosols based on aerosol mass spectrometry, *Environ. Sci. Technol.*, *39*, 4938–4952, doi:4910.1021/es048568l.

Zhang, Q., D. R. Worsnop, M. R. Canagaratna, and J. L. Jiménez (2005b), Hydrocarbon-like and oxygenated organic aerosols in Pittsburgh: Insights into sources and processes of organic aerosols, *Atmos. Chem. Phys.*, *5*, 3289–3311.

Zhang, Q., et al. (2007), Ubiquity and dominance of oxygenated species in organic aerosols in anthropogenically-influenced Northern Hemisphere mid-latitudes, *Geophys. Res. Lett.*, *34*, L13801, doi:10.1029/2007GL029979.

M. R. Canagaratna, S. C. Herndon, J. T. Jayne, C. E. Kolb, J. H. Kroll, T. B. Onasch, E. C. Wood, and D. R. Worsnop, Aerodyne Research, Inc., 45 Manning Road, Billerica, MA 01821-3976, USA. (mrcana@aerodyne.com; herndon@aerodyne.com; jayne@aerodyne.com; kolb@aerodyne.com; kroll@aerodyne.com; onasch@aerodyne.com; ezrawood@aerodyne.com; worsnop@aerodyne.com)

B. de Foy, Department of Earth and Atmospheric Sciences, Saint Louis University, 221 North Grand Boulevard, St. Louis, MO 63103, USA. (bdefoy@slu.edu)

J. A. de Gouw, Earth System Research Laboratory, R/CSD7, NOAA, 325 Broadway, Boulder, CO 80305, USA. (joost.degouw@noaa.gov)

M. K. Dubey and C. Mazzoleni, Earth and Environmental Sciences Division, Los Alamos National Laboratory, MS D462, Los Alamos, NM 87545, USA. (dubey@lanl.gov; claudio@lanl.gov)

J. Fast, Pacific Northwest National Laboratory, P.O. Box 999, MSIN K9-30, Richland, WA 99352, USA. (jerome.fast@pnl.gov)

J. L. Jimenez and I. M. Ulbrich, Department of Chemistry and Biochemistry and CIRES, University of Colorado, UCB 216, Boulder, CO 80309-0216, USA. (jose.jimenez@colorado.edu; ingrid.ulbrich@colorado.edu)

W. B. Knighton, Department of Chemistry and Biochemistry, Montana State University, P.O. Box 173400, Bozeman, MT 59717, USA. (bknighton@chemistry.montana.edu)

L. T. Molina and M. A. Zavala, Molina Center for Energy and the Environment, 3262 Holiday Court, Suite 201, La Jolla, CA 92037, USA. (ltmolina@mit.edu; miguelz@mit.edu)

R. Seila, National Exposure Research Laboratory, Environmental Protection Agency, Research Triangle Park, NC 27711, USA. (seila.robert@epamail.epa.gov)